

Synthesis of $N(\text{SiMe}_3)_2$ supported vanadium(III) complexes, including hydrocarbyl, tetrahydroborate and azaalkenyldene derivatives†

Christopher P. Gerlach and John Arnold*

Department of Chemistry, University of California, Berkeley, California 94720-1460, USA

Reaction of $[(\text{Me}_3\text{Si})_2\text{N}]_2\text{VCl}(\text{THF})$ (THF = tetrahydrofuran) with MgMe_2 or LiMe afforded $[(\text{Me}_3\text{Si})_2\text{N}]_2\text{VMe}(\text{THF})$ in 70% yield. Nitrogen donors displaced THF in these V^{III} species, and $[(\text{Me}_3\text{Si})_2\text{N}]_2\text{VCl}(\text{lut})$ (lut = 3,5-dimethylpyridine) and $[(\text{Me}_3\text{Si})_2\text{N}]_2\text{VMe}(\text{pyr})$ (pyr = pyridine) were isolated and characterized. Solution thermolysis of $[(\text{Me}_3\text{Si})_2\text{N}]_2\text{VMe}(\text{THF})$ yielded the known V^{III} dimer $\{[(\text{Me}_3\text{Si})_2\text{N}]\text{V}(\mu\text{-CH}_2\text{SiMe}_2\text{-NSiMe}_3)\}_2$ in 73% yield. Reaction of $[(\text{Me}_3\text{Si})_2\text{N}]_2\text{VMe}(\text{THF})$ with 3 equivalents of RNC ($\text{R} = \text{Bu}^t$ or Xyl; Xyl = 2,6-dimethylphenyl) gave diazavanadacycles of empirical formulae $[(\text{Me}_3\text{Si})_2\text{N}]_2\text{V}[(\text{Me})(\text{CNR})_3]$. For $\text{R} = \text{Bu}^t$, the product $[(\text{Me}_3\text{Si})_2\text{N}]_2\text{V}[\text{Bu}^t\text{N}=\text{CMeC}(\text{C}=\text{NBu}^t)\text{NBu}^t]$ features an exocyclic keteneamine functionality; for $\text{R} = \text{Xyl}$, an additional C–C bond forming step results in slightly more complex connectivity, to give $[(\text{Me}_3\text{Si})_2\text{N}]_2\text{V}[(\text{Xyl})\text{CMe}=\text{C}(\text{C}=\text{NXyl})\text{CMeCH}=\text{CH}-\text{CH}=\text{CMeC}(\text{C}=\text{N})]$. The crystal structures of both compounds are presented. Alkylation of $[(\text{Me}_3\text{Si})_2\text{N}]_2\text{VCl}(\text{THF})$ with 2-thienyllithium led to isolation of $[(\text{Me}_3\text{Si})_2\text{N}]_2\text{V}(2\text{-C}_4\text{H}_5\text{S})(\text{THF})$ (60%). A blue solution that acted as a source of $[(\text{Me}_3\text{Si})_2\text{N}]_2\text{VPh}$ was obtained from the reaction of 0.5 equivalent of MgPh_2 with $[(\text{Me}_3\text{Si})_2\text{N}]_2\text{VCl}(\text{THF})$. The addition of pyr or PhCN to the blue mixture gave $[(\text{Me}_3\text{Si})_2\text{N}]_2\text{VPh}(\text{pyr})$ (60%) and $[(\text{Me}_3\text{Si})_2\text{N}]_2\text{V}(\text{NCPh}_2)(\text{NCPh})$ (66%), respectively. The chelated aryl amine $[(\text{Me}_3\text{Si})_2\text{N}]_2\text{V}(o\text{-Me}_2\text{NCH}_2\text{C}_6\text{H}_4)$ was synthesized from $[(\text{Me}_3\text{Si})_2\text{N}]_2\text{VCl}(\text{THF})$ and $\text{Li}(o\text{-Me}_2\text{NCH}_2\text{C}_6\text{H}_4)$ in 81% yield. Treatment of $[(\text{Me}_3\text{Si})_2\text{N}]_2\text{VCl}(\text{THF})$ with excess LiBH_4 in the presence of pyr afforded the vanadium tetrahydroborate $[(\text{Me}_3\text{Si})_2\text{N}]_2\text{V}(\eta^2\text{-BH}_4)(\text{THF})$ in 41% yield. The solid-state structures of $[(\text{Me}_3\text{Si})_2\text{N}]_2\text{VPh}(\text{pyr})$, $[(\text{Me}_3\text{Si})_2\text{N}]_2\text{V}(\text{NCPh}_2)(\text{NCPh})$, $[(\text{Me}_3\text{Si})_2\text{N}]_2\text{V}(\eta^2\text{-}o\text{-Me}_2\text{NCH}_2\text{C}_6\text{H}_4)$ and $[(\text{Me}_3\text{Si})_2\text{N}]_2\text{V}(\eta^2\text{-BH}_4)(\text{pyr})$ are reported.

We recently reported the syntheses and structures of three-coordinate vanadium chalcogenolates of the form $[(\text{Me}_3\text{Si})_2\text{N}]_2\text{V-ER}$ [$\text{E} = \text{Se}$ or Te ; $\text{R} = \text{Si}(\text{SiMe}_3)_3$ or SiPh_3]¹ and demonstrated that in addition to being electrophilic by virtue of their electron-deficient, co-ordinatively unsaturated nature, they are susceptible to two-electron oxidation reactions. Based on these results, we thought it worthwhile to pursue the preparation of three-coordinate alkyl, aryl or hydride species *i.e.* $[(\text{Me}_3\text{Si})_2\text{N}]_2\text{VR}$, particularly since little is known about organovanadium chemistry in non-cyclopentadienyl environments.² Unfortunately, isolation of species of this type was hindered by metallation of a bis(trimethylsilyl)amide ligand.^{3–7} Nonetheless, facile loss of tetrahydrofuran (THF) from $[(\text{Me}_3\text{Si})_2\text{N}]_2\text{VR}(\text{THF})$ ($\text{R} = \text{Me}$ or Ph), while posing certain steric constraints on R, enabled these molecules to act as sources of $[(\text{Me}_3\text{Si})_2\text{N}]_2\text{VR}$ fragments, much in the way $(\text{Mes})_3\text{V}(\text{THF})$ ($\text{Mes} = 2,4,6\text{-Me}_3\text{C}_6\text{H}_2$)^{8,9} is an effective source of $\text{V}(\text{Mes})_3$.^{10–12} Thus, we have explored the reactivity of $[(\text{Me}_3\text{Si})_2\text{N}]_2\text{VR}(\text{THF})$ with a variety of reagents containing $\text{C}\equiv\text{N}$, $\text{C}\equiv\text{C}$ and $\text{C}=\text{O}$ bonds and the results are presented herein. Substitution of chloride in $[(\text{Me}_3\text{Si})_2\text{N}]_2\text{VCl}(\text{THF})$ for 2-thienyl, tetrahydroborate and *o*-dimethylaminomethylphenyl was also carried out and crystal structures of the latter two products are presented.

Experimental

General

Standard inert atmosphere glovebox and Schlenk-line techniques were employed for all manipulations. All solvents were predried over 4 Å molecular sieves and in the case of C_6D_6 , hexanes, diethyl ether and THF, were distilled from sodium-benzophenone under N_2 . Toluene, pyridine (pyr), hexamethyl-

disiloxane (HMDSO) and 3,5-dimethylpyridine (lut) were distilled from sodium while benzonitrile was distilled from CaH_2 . The compounds $[(\text{Me}_3\text{Si})_2\text{N}]_2\text{VCl}(\text{THF})$,^{13,14} MgMe_2 ,¹⁵ MgPh_2 ,¹⁵ $\text{Li}(o\text{-Me}_2\text{NCH}_2\text{C}_6\text{H}_4)$ ¹⁶ and $\text{Li}(2\text{-C}_4\text{H}_5\text{S})$ ¹⁷ were synthesized by literature procedures. Methyllithium (1.4 M, Et_2O), LiBH_4 , CNXyl (Xyl = 2,6-dimethylphenyl), and CNBu^t were purchased from commercial suppliers. Samples for IR spectroscopy were prepared as mineral oil mulls between KBr plates. Melting points were determined under N_2 in sealed capillary tubes. Proton NMR spectra were recorded in C_6D_6 on a 300 MHz spectrometer at ambient temperature. Magnetic susceptibility measurements were made by the method of Evans^{18,19} in C_6D_6 and the values reported are uncorrected. The C, H and N analyses were done within the College of Chemistry, University of California, Berkeley. X-Ray data were collected and the structures solved at the University of California at Berkeley, X-ray facility.

$[(\text{Me}_3\text{Si})_2\text{N}]_2\text{VMe}(\text{THF})$

Method A. Dimethylmagnesium (440 mg, 8.09 mmol) and $[(\text{Me}_3\text{Si})_2\text{N}]_2\text{VCl}(\text{THF})$ (7.76 g, 16.2 mmol) were mixed with THF (100 mL) giving a deep blue solution. After 20 min, the volatile materials were removed under reduced pressure, the blue solid extracted with hexanes (2×200 mL; 100 mL), and the extracts filtered through a frit padded with Celite. The blue filtrate was concentrated to *ca.* 80 mL and cooled to -25°C for 24 h. Blue crystals were isolated by filtration (4.93 g, 67%) and dried under vacuum.

Method B. An ether solution (30 mL) of $[(\text{Me}_3\text{Si})_2\text{N}]_2\text{VCl}(\text{THF})$ (1.65 g, 3.44 mmol) was treated with LiMe (2.46 mL, 3.44 mmol) giving a deep blue solution. After stirring for 8 h, work-up as in method A afforded 1.19 g (75%) of blue crystals. M.p. $95\text{--}98^\circ\text{C}$ (decomp.). IR: 1256 (sh), 1245s, 1172w, 1154w, 1038w, 1012m, 936vs, 890m, 848vs, 781s, 754m, 723m,

† Non-SI units employed: $\mu_B \approx 9.27 \times 10^{-24} \text{ J T}^{-1}$, atm = 101 325 Pa.

696m, 667s, 636m, 614m, 496m cm^{-1} . $\mu = 2.72 \mu_{\text{B}}$ (Found: C, 44.37; H, 10.27; N, 5.94. Calc. for $\text{C}_{17}\text{H}_{47}\text{N}_2\text{OSi}_4\text{V}$: C, 44.50; H, 10.32; N, 6.11%).

Thermolysis of $[(\text{Me}_3\text{Si})_2\text{N}]_2\text{VMe}(\text{THF})$

A hexanes solution (30 mL) of $[(\text{Me}_3\text{Si})_2\text{N}]_2\text{VMe}(\text{THF})$ (431 mg, 0.939 mmol) was heated under an Ar(g) atmosphere with an oil bath that was brought up to 80 °C for 5 min. The mixture turned from blue to violet and was cooled to room temperature. The volatile materials were removed under reduced pressure, the solid was extracted into toluene (25 mL) and the solution filtered. Concentration of the filtrate to *ca.* 10 mL followed by cooling to -25°C for 16 h afforded 253 mg (73%) of violet crystals of $\{[(\text{Me}_3\text{Si})_2\text{N}]\text{V}(\eta^2\text{-CH}_2\text{SiMe}_2\text{NSiMe}_3)\}_2$ that were isolated by filtration and dried under vacuum. The compound was characterized by comparison of its physical and spectroscopic data to both the literature data¹³ and to those of an independent sample prepared *via* the literature route. Although the material is paramagnetic, several low intensity resonances in the ^1H NMR spectrum are characteristic. ^1H NMR (300 MHz, C_6D_6): δ 0.96, 0.64, 0.39, 0.21, -1.2 .

$[(\text{Me}_3\text{Si})_2\text{N}]_2\text{VMe}(\text{pyr})$

Method A. Pyridine (156 μL , 1.93 mmol) was added to a hexanes solution (30 mL) of $[(\text{Me}_3\text{Si})_2\text{N}]_2\text{VMe}(\text{THF})$ (881 mg, 1.92 mmol) affording a green mixture that was stirred for 4 h. The volatile materials were then removed under reduced pressure, the solid extracted with hexanes (35 mL), and the solution filtered. Concentration of the filtrate to *ca.* 5 mL followed by cooling overnight to -25°C yielded dark green crystals that were isolated by filtration and dried under vacuum (659 mg, 74%).

Method B. The compounds $[(\text{Me}_3\text{Si})_2\text{N}]_2\text{VCl}(\text{THF})$ (1.11 g, 2.32 mmol) and Me_2Mg (63 mg, 1.2 mmol) were mixed with THF (30 mL). After 5 min, the blue solution was treated with pyr (225 μL , 2.78 mmol) turning it dark green. An analogous work-up as in method A afforded 570 mg (53%) of product that was isolated by filtration and dried under vacuum. M.p. 89–92 °C. ^1H NMR (0.12 M): δ 2.7 ($\Delta\nu_i$ *ca.* 380 Hz). IR: 1602m, 1483m, 1444s, 1247vs, 1213m, 1170w, 1153m, 1125w, 1067m, 1044m, 1011m, 936vs, 879s, 848vs, 782s, 752s, 695s, 666s, 638m, 628m, 614m, 488m cm^{-1} . $\mu = 2.71 \mu_{\text{B}}$ (Found: C, 45.37; H, 9.60; N, 8.90. Calc. for $\text{C}_{18}\text{H}_{44}\text{N}_3\text{Si}_4\text{V}$: C, 46.41; H, 9.52, N, 9.02%).

$[(\text{Me}_3\text{Si})_2\text{N}]_2\text{VCl}(\text{lut})$

3,5-Dimethylpyridine (210 μL , 1.84 mmol) was added to a hexanes solution (30 mL) of $[(\text{Me}_3\text{Si})_2\text{N}]_2\text{VCl}(\text{THF})$ (843 mg, 1.76 mmol). The resulting orange mixture was stirred for 1 h and then the volatiles were removed under reduced pressure. The residue was extracted with hexanes (40 mL), the solution filtered, and the solvent removed under reduced pressure. This solid was then extracted with HMDSO (60 mL), filtered, and the orange filtrate concentrated to *ca.* 10 mL. Cooling to -25°C for 24 h afforded 450 mg (50%) of dark (purple) needles that were isolated by filtration and dried under vacuum. M.p. 94–95 °C (decomp.). ^1H NMR (0.11 M): δ 2.8 ($\Delta\nu_i$ *ca.* 400 Hz). IR: 1597w, 1258 (sh), 1247s, 1148m, 1018m, 919s, 879m, 847s, 782m, 757m, 722m, 701 (sh), 694m, 667m, 635w, 616w cm^{-1} . $\mu = 2.74 \mu_{\text{B}}$ (Found: C, 44.25; H, 8.83; N, 8.12. Calc. for $\text{C}_{19}\text{H}_{45}\text{ClN}_3\text{Si}_4\text{V}$: C, 44.37; H, 8.82; N, 8.17%).

$[(\text{Me}_3\text{Si})_2\text{N}]_2\text{V}(2\text{-C}_4\text{H}_3\text{S})(\text{THF})$

The compounds $[(\text{Me}_3\text{Si})_2\text{N}]_2\text{VCl}(\text{THF})$ (557 mg, 1.16 mmol) and $\text{Li}(\text{C}_4\text{H}_3\text{S})\cdot 1.5\text{THF}$ (230 mg, 1.16 mmol) were mixed with THF (30 mL) giving a blue-green mixture. After stirring for 24 h, the volatile materials were removed under reduced pressure leaving a green residue that was extracted with hexanes (40

mL). Following filtration, the solution was concentrated and cooled to -25°C . The product was isolated in two crops as dark (blue-green) crystals (366 mg, 60%) that were dried under vacuum. M.p. 98–102 °C (decomp.). IR: 1599w, 1306w, 1246s, 1189w, 1174m, 1042m, 1006w, 982m, 929s, 911s, 885s, 848vs, 783m, 759m, 721m, 698m, 666m, 643w, 615w cm^{-1} . $\mu = 2.61 \mu_{\text{B}}$ (Found: C, 45.94; H, 8.91; N, 5.04. Calc. for $\text{C}_{20}\text{H}_{47}\text{N}_2\text{OSSi}_4\text{V}$: C, 45.59; H, 8.99; N, 5.32%).

Hydrolysis of $[(\text{Me}_3\text{Si})_2\text{N}]_2\text{V}(2\text{-C}_4\text{H}_3\text{S})(\text{THF})$

The compound $[(\text{Me}_3\text{Si})_2\text{N}]_2\text{V}(2\text{-C}_4\text{H}_3\text{S})(\text{THF})$ (20 mg, 0.038 mmol) was dissolved in *ca.* 0.5 mL of C_6D_6 . The sample was treated with H_2O (7.0 μL , 0.39 mmol, N_2 -degassed) and the mixture became clear yellow with some brown precipitate. Analysis by ^1H NMR spectroscopy showed (along with excess H_2O) only $\text{HN}(\text{SiMe}_3)_2$, THF and thiophene in a 2:1:1 ratio, respectively.

$[(\text{Me}_3\text{Si})_2\text{N}]_2\text{V}[\text{Bu}'\text{N}=\text{CMeC}(\text{C}=\text{NBu}')\text{NBu}']$

A cold (-40°C) hexanes solution of $[(\text{Me}_3\text{Si})_2\text{N}]_2\text{VMe}(\text{THF})$ (352 mg, 0.767 mmol) was treated with CNBu' (260 μL , 2.30 mmol). The mixture was gradually warmed to ambient temperature after which it was golden red. The volatile materials were removed under reduced pressure and the red solid extracted with HMDSO (40 mL) and then hexanes (35 mL). The combined filtrates were concentrated to *ca.* 15 mL and cooled to -25°C for 48 h. Dark red crystals were isolated by filtration and dried under vacuum (339 mg, 69%). The powdered compound is green. M.p. 128–130 °C (decomp.). ^1H NMR (0.07 M): δ 1.2 ($\Delta\nu_i$ *ca.* 45 Hz). IR: 1987vs, 1518m, 1325m, 1243m, 1204m, 1193m, 1180m, 1126w, 1028w, 1002w, 940 (sh), 904vs, 873s, 849s, 781m, 756w, 699m, 671m, 628m, 565m, 544m cm^{-1} . $\mu = 2.79 \mu_{\text{B}}$ (Found: C, 53.04; H, 10.43; N, 10.92. Calc. for $\text{C}_{28}\text{H}_{66}\text{N}_5\text{Si}_4\text{V}$: C, 52.87; H, 10.46; N, 11.01%).

$[(\text{Me}_3\text{Si})_2\text{N}]_2\text{V}[\text{N}(\text{Xyl})\text{C}(\text{Me})=\text{CC}(\text{C}=\text{NXyl})\text{CMeCH}=\text{CHCH}=\text{C}(\text{Me})\text{C}(\text{N})]$

Toluene was added to a mixture of $[(\text{Me}_3\text{Si})_2\text{N}]_2\text{VMe}(\text{THF})$ (364 mg, 0.793 mmol) and CNXyl (312 mg, 2.38 mmol). Over a few minutes the mixture became violet. After 4 h, the volatile materials were removed under reduced pressure and the dark solid was extracted with hexanes (2×40 mL). The filtrate was concentrated to *ca.* 20 mL and cooled to -25°C . After 24 h, the product was isolated by filtration as dark purple crystals (464 mg, 75%) that were dried under vacuum. M.p. 165–167 °C (decomp.). IR: 1636s, 1594m, 1562vs, 1543m (sh), 1335s, 1296w, 1274m, 1250s, 1224m, 1207m, 1189m, 1168w, 1160w, 1140w, 1090w, 1034w, 987w, 973w, 953w, 927m, 911s, 882vs, 850vs, 784m, 762m, 741 (sh), 735m, 721m, 709m, 700m, 680 (sh), 665m, 636m, 618w, 572w, 530w, 503w, 485w, 471w cm^{-1} . $\mu = 2.81 \mu_{\text{B}}$ (Found: C, 61.68; H, 8.50; N, 8.89. Calc. for $\text{C}_{40}\text{H}_{66}\text{N}_5\text{Si}_4\text{V}$: C, 61.57; H, 8.53; N, 8.98%).

$[(\text{Me}_3\text{Si})_2\text{N}]_2\text{VPh}(\text{pyr})$

The compounds $[(\text{Me}_3\text{Si})_2\text{N}]_2\text{VCl}(\text{THF})$ (592 mg, 1.24 mmol) and MgPh_2 (110 mg, 0.616 mmol) were mixed with THF (25 mL) giving a blue solution. Pyridine (105 μL , 1.30 mmol) was added turning the mixture green. After 15 min, the volatile materials were removed under reduced pressure and the green solid extracted with hexanes (2×25 mL). The green/red dichroic filtrate was concentrated to *ca.* 20 mL and cooled to -25°C for 24 h. The product was isolated in two crops by filtration and dried under vacuum (395 mg, 60%). M.p. 106–108 °C (decomp.). IR: 1603m, 1444s, 1260m, 1245s, 1213w, 1154w, 1065w, 1054w, 1044w, 948m, 926s, 878s, 845s, 818 (sh), 782m, 754m, 722m, 697s, 665m, 636w, 628w, 616w cm^{-1} . $\mu = 2.75 \mu_{\text{B}}$ (Found: C, 52.10; H, 8.74; N, 7.89. Calc. for $\text{C}_{23}\text{H}_{46}\text{N}_3\text{Si}_4\text{V}$: C, 52.33; H, 8.78; N, 7.96%).

$[(\text{Me}_3\text{Si})_2\text{N}]_2\text{V}(\text{NCPh})(\text{NCPh})$

The compounds $[(\text{Me}_3\text{Si})_2\text{N}]_2\text{VCl}(\text{THF})$ (1.01 g, 2.11 mmol) and MgPh_2 (188 mg, 1.05 mmol) were mixed with THF (20 mL) giving a blue solution. After 2 h, PhCN (0.65 mL, 6.4 mmol) was added turning the mixture red-brown. After 12 h, the volatile materials were removed under reduced pressure and the solid was extracted with hexanes (2×35 mL). Concentration of the filtrate to *ca.* 20 mL and cooling to -25°C for 24 h afforded 915 mg (66%) of burgundy crystals that were isolated by filtration and dried under vacuum. M.p. $100\text{--}102^\circ\text{C}$ (decomp.). ^1H NMR (0.04 M): δ 3.8 ($\Delta\nu$ *ca.* 425 Hz). IR: 2236w, 1596w, 1498w, 1243s, 1200w, 1176w, 1029w, 956 (sh), 934vs, 876vs, 845vs, 778s, 757s, 695s, 665m, 627m, 615w, 550m, 483w cm^{-1} . $\mu = 2.67 \mu_{\text{B}}$ (Found: C, 58.60; H, 7.84; N, 8.59. Calc. for $\text{C}_{32}\text{H}_{51}\text{N}_4\text{Si}_4\text{V}$: C, 58.67; H, 7.85; N, 8.55%).

$[(\text{Me}_3\text{Si})_2\text{N}]_2\text{V}(\eta^2\text{-C}_6\text{H}_4\text{CH}_2\text{NMe}_2)$

The compounds $[(\text{Me}_3\text{Si})_2\text{N}]_2\text{VCl}(\text{THF})$ (974 mg, 2.03 mmol) and $\text{LiC}_6\text{H}_4\text{CH}_2\text{NMe}_2$ (287 mg, 2.03 mmol) were mixed with THF (30 mL) giving a deep blue solution. After 1 h, the volatile materials were removed under reduced pressure and the blue solid was extracted with hexanes (30 mL). Concentration of the filtrate to *ca.* 15 mL followed by slowly cooling to -25°C afforded 281 mg (27%) of blue crystals that were isolated by filtration and dried under vacuum. The filtrate was stripped to dryness affording an additional 555 mg of product as a blue powder (net yield 81%). M.p. $120\text{--}121^\circ\text{C}$ (decomp.). IR: 1257 (sh), 1246s, 1017w, 985m, 965m, 917s, 881s, 840s, 781s, 755m, 739s, 722m, 694m, 665s, 632m, 613w, 505w, 489w cm^{-1} . $\mu = 2.77 \mu_{\text{B}}$ (Found: C, 49.82; H, 9.63; N, 8.32. Calc. for $\text{C}_{21}\text{H}_{48}\text{N}_3\text{Si}_4\text{V}$: C, 49.86; H, 9.56; N, 8.31%).

$[(\text{Me}_3\text{Si})_2\text{N}]_2\text{V}(\eta^2\text{-BH}_4)(\text{pyr})$

The compounds $[(\text{Me}_3\text{Si})_2\text{N}]_2\text{VCl}(\text{THF})$ (2.91 g, 6.07 mmol) and LiBH_4 (397 mg, 18.2 mmol) were mixed with Et_2O (40 mL) giving a blue mixture. The reaction was stirred for 8 h, filtered, and then pyr (0.98 mL, 12.1 mmol) was added turning the solution dark orange-brown. After stirring for a further 15 min, the volatile materials were removed under reduced pressure. The red-brown solid was extracted with hexanes (2×60 mL) and the filtrate concentrated to *ca.* 40 mL. After cooling to -25°C for 24 h, red-brown crystals were isolated by filtration (1.17 g, 41%) and dried under vacuum. The material is green in powdered form. M.p. $98\text{--}101^\circ\text{C}$ (decomp.). ^1H NMR (0.08 M): δ 3.5 ($\Delta\nu$ *ca.* 830 Hz). IR: 2453m, 2402m, 2246w, 2141m, 1605m, 1249s, 1216m, 1156w, 1129m, 1068m, 1046m, 1010m, 912vs, 877s, 838vs, 782s, 754s, 691m, 664m, 641m, 629m, 616m, 445m, 426m cm^{-1} . $\mu = 2.78 \mu_{\text{B}}$ (Found: C, 43.51; H, 9.74; N, 9.09. Calc. for $\text{C}_{17}\text{H}_{43}\text{BN}_3\text{Si}_4\text{V}$: C, 43.85; H, 9.74; N, 9.02%).

X-Ray crystallography

A summary of crystal data, data collection and refinement for all crystallographically characterized compounds is given in Table 1. Selected metrical data are presented in Table 2.

$[(\text{Me}_3\text{Si})_2\text{N}]_2\text{VPh}(\text{pyr})$. Green crystals were grown from a concentrated hexanes solution at -25°C . A suitable crystal was mounted on a glass capillary under Paratone-N hydrocarbon oil. The crystal was transferred to a Siemens SMART diffractometer/CCD area detector²⁰ and cooled by a nitrogen-flow, low-temperature apparatus which had been previously calibrated by a thermocouple placed at the same position as the crystal. A preliminary orientation matrix and unit-cell parameters were determined by collecting 60, 10 s frames, followed by spot integration and least-squares refinement. A hemisphere of data was collected using $0.3^\circ \omega$ scans at 10 s per frame. The raw data were integrated (XY spot spread = 1.60° ; Z spot

spread = 0.60°) and the unit cell parameters refined [8192 reflections with $I > 10\sigma(I)$] using SAINT.²¹ The intensity statistics were consistent with a centrosymmetric space group, and the space group $P2_1/c$ (no. 14) was uniquely defined by the systematic absences. The data were corrected for Lorentz-polarization effects, but no correction for crystal decay or absorption was applied to the data. Of the 12922 reflections measured, 4673 were unique and 3338 had $I > 3\sigma(I)$ and were used in the refinement. Redundant reflections ($R_{\text{int}} = 0.0343$) were averaged. The structure was solved by direct methods using the TEXSAN²² package on a Digital microvax workstation, and refined using standard least-squares and Fourier techniques. All non-hydrogen atoms were refined with anisotropic thermal parameters; hydrogen atoms were located from the difference map and refined with isotropic thermal parameters. Anomalous thermal parameters for C(13) and N(3) suggested disorder between the phenyl and pyridine ligands. A model in which the combined electron density at these two positions was constrained to equal a total of 13 electrons (*i.e.* 1 carbon + 1 nitrogen) refined with lower R values and more acceptable thermal parameters for both atoms. The refined occupancies [C(13) 1.027; N(3) 0.973] imply that the disorder between the two sites is of the order of 25%, rather than the 50% value expected if these positions were totally disordered. Neutral atomic scattering factors were taken from Cromer and Waber²³ and anomalous dispersion effects were included in F_c .²⁴ The final residuals for 465 variables refined against 3338 data for which $I > 3\sigma(I)$ were $R = 0.0346$, $R' = 0.0446$ and $S = 1.762$.

$[(\text{Me}_3\text{Si})_2\text{N}]_2\text{V}(\text{NCPh})(\text{NCPh})$. The collection and preliminary treatment of data were as described above. Due to a mishap with the crystal cooling apparatus that resulted in the temperature warming to 17°C during the initial portion of the data collection, the first 100 frames of data were not used for the structure solution. The space group $P\bar{1}$ was indicated by the absence of any higher symmetry and the intensity statistics were consistent with a centric space group. The structure was solved as described above. A rotational disorder about the Si(1)–N(1) vector resulted in partial occupancies of 0.62 for C(1)–C(3). The carbon atoms of the minor rotomer [C(33)–C(35)] were constrained to sum to full occupancy. All full-occupancy, non-hydrogen atoms were refined with anisotropic thermal parameters. Hydrogen atoms associated with the ordered SiMe_3 groups were assigned to idealized positions and were included in F_c but not refined. The final residuals for 368 variables refined against 3653 data for which $I > 3\sigma(I)$ were $R = 0.0748$, $R' = 0.01082$ and $S = 3.569$.

$[(\text{Me}_3\text{Si})_2\text{N}]_2\text{V}(\eta^2\text{-}o\text{-Me}_2\text{NCH}_2\text{C}_6\text{H}_4)$. All aspects, from data collection through the solution and refinement of the structure, were as described for $[(\text{Me}_3\text{Si})_2\text{N}]_2\text{VPh}(\text{pyr})$. Intensity statistics indicated a centrosymmetric space group and the structure was solved successfully in $P\bar{1}$. The final residuals for 454 variables refined against 3724 data for which $I > 3\sigma(I)$ were $R = 0.0333$, $R' = 0.0470$ and $S = 1.96$.

$[(\text{Me}_3\text{Si})_2\text{N}]_2\text{V}(\text{Me})(\text{CNBu}^t)_3$. All aspects, from the data collection through the solution and refinement of the structure, were as described for $[(\text{Me}_3\text{Si})_2\text{N}]_2\text{VPh}(\text{pyr})$, except in the present case the hydrogen atoms were assigned to fixed, idealized positions. The space group $P2_1/n$ was uniquely defined by the systematic absences. The final residuals for 343 variables refined against 4137 data for which $I > 3\sigma(I)$ were $R = 0.0393$, $R' = 0.0528$ and $S = 1.93$.

$[(\text{Me}_3\text{Si})_2\text{N}]_2\text{V}(\text{Me})(\text{CNXyl})_3$. The data collection, solution, and refinement of this structure were the same as indicated for the CNBu^t analog above. The space group $P2_1/n$ was uniquely defined by the systematic absences. The final residuals for 451

Table 1 Summary of X-ray diffraction data {[N] = N(SiMe₃)₂}

	[N] ₂ VPh(pyr)	[N] ₂ V(NCPh ₂)(NCPh)	[N] ₂ V(η ² -C ₆ H ₄ CH ₂ NMe ₂)	[N] ₂ V[(Me)(CNBu ^t) ₃]	[N] ₂ V[(Me)(CNXyl) ₃]	[N] ₂ V(η ² -BH ₄)(pyr)
Formula	C ₂₃ H ₄₆ N ₃ Si ₄ V	C ₃₂ H ₅₁ N ₄ Si ₄ V	C ₂₁ H ₄₈ N ₃ Si ₄ V	C ₂₈ H ₆₆ N ₅ Si ₄ V	C ₄₀ H ₆₆ N ₅ Si ₄ V	C ₁₇ H ₄₅ BN ₃ Si ₄ V
<i>M</i>	527.92	655.07	505.91	636.15	780.28	465.66
Source, color, habit	Hexanes, green, tabular	Hexanes, blue, equant	Hexanes, blue, equant	HMDSO, red, equant	Toluene, purple, tabular	Hexanes, brown, equant
Crystal size/mm	0.40 × 0.30 × 0.15	0.38 × 0.29 × 0.27	0.50 × 0.41 × 0.30	0.44 × 0.34 × 0.25	0.25 × 0.15 × 0.05	0.36 × 0.30 × 0.20
Crystal system	Monoclinic	Triclinic	Triclinic	Monoclinic	Monoclinic	Monoclinic
Space group	<i>P</i> 2 ₁ / <i>c</i>	<i>P</i> $\bar{1}$	<i>P</i> $\bar{1}$	<i>P</i> 2 ₁ / <i>n</i>	<i>P</i> 2 ₁ / <i>n</i>	<i>P</i> 2 ₁ / <i>c</i>
<i>T</i> /°C	−115	17	−117	−118	−105	−114
<i>a</i> /Å	13.2248(2)	9.2055(2)	8.8835(2)	17.2448(3)	10.4622(5)	17.6053(3)
<i>b</i> /Å	11.7152(1)	11.49242(2)	11.7690(1)	11.2213(2)	20.3892(10)	8.4737(1)
<i>c</i> /Å	19.8869(1)	19.2860(4)	14.6715(3)	20.8749(2)	20.7733(10)	18.6582(4)
<i>α</i> /°		89.195(1)	92.799(1)			
<i>β</i> /°	99.184(1)	87.266(1)	92.572(1)	107.325(1)	96.250(1)	98.819(1)
<i>γ</i> /°		71.647(1)	103.295(1)			
<i>U</i> /Å ³	3081.08(4)	1934.33(9)	1488.54(6)	3856.23(13)	4404.93	2750.54(12)
<i>Z</i>	4	2	2	4	4	4
<i>ρ</i> _{calc} /g cm ^{−3}	1.14	1.12	1.13	1.10	1.18	1.12
<i>μ</i> /cm ^{−1}	4.92	4.05	5.06	4.04	3.67	6.4
Radiation (λ/Å)	Mo-Kα (0.710 73)	Mo-Kα (0.710 73)	Mo-Kα (0.710 73)	Mo-Kα (0.710 73)	Mo-Kα (0.710 73)	Mo-Kα (0.710 73)
Scan mode	ω (0.3° scans)	ω (0.3° scans)	ω (0.3° scans)	ω (0.3° scans)	ω (0.3° scans)	ω (0.3° scans)
2θ Range/°	3–45	3–45	3–45	3–45	3–45	3–45
Total no. reflections	12922	7263	6157	16293	18426	11397
No. unique reflections	4673	5103	4165	5875	6535	4240
<i>R</i> _{int}	0.0343	0.0932	0.0248	0.0344	0.057	0.029
Absorption type	None	Semiempirical, XPREP	Semiempirical, XPREP	Semiempirical, XPREP	Semiempirical, XPREP	Semiempirical, XPREP
Transmittance coefficient	NA	0.524–0.871	0.783–0.852	0.768–0.898	0.897–0.974	0.799–0.893
No. of observations (<i>n</i> _o), <i>I</i> > 3σ(<i>I</i>)	3338	3653	3724	4137	3773	3123
No. of parameters refined (<i>n</i> _v)	465	368	454	343	451	236
Final <i>R</i> , ^a <i>R'</i> ^b	0.0346, 0.0446	0.0748, 0.1082	0.0333, 0.0470	0.0393, 0.0528	0.0432, 0.0518	0.0306, 0.0422
<i>S</i> ^c	1.76	3.57	1.96	1.93	1.57	1.63

^a *R* = [Σ||*F*_o| − |*F*_c||]/Σ|*F*_o|. ^b *R'* = {[Σ_w(|*F*_o| − |*F*_c||)²]/Σ_w*F*_o²}^{1/2}. ^c *S* = [Σ_w(|*F*_o|² − |*F*_c|²)/(*n*_o − *n*_v)]^{1/2}.

Table 2 Selected metrical data for crystallographically characterized compounds, bond lengths in Å, angles in °

[(Me ₃ Si) ₂ N] ₂ V[Bu ^t N=CMeC(=C=NBu ^t)NBu ^t]							
V–N(1)	1.998(3)	V–N(4)	1.921(2)	N(5)–C(25)	1.205(4)	C(26)–C(27)	1.446(4)
V–N(2)	2.014(3)	N(3)–C(27)	1.316(4)	C(25)–C(26)	1.345(4)	C(27)–C(28)	1.507(5)
V–N(3)	2.098(3)	N(4)–C(26)	1.402(4)				
N(1)–V–N(2)	123.5(1)	N(2)–V–N(3)	101.9(1)	V–N(3)–C(27)	112.3(2)	N(4)–C(26)–C(27)	116.2(3)
N(1)–V–N(3)	116.5(1)	N(2)–V–N(4)	118.0(1)	V–N(4)–C(26)	114.2(2)	N(5)–C(25)–C(26)	171.7(3)
N(1)–V–N(4)	107.6(1)	N(3)–V–N(4)	81.6(1)	N(3)–C(27)–C(26)	115.2(3)		
[(Me ₃ Si) ₂ N] ₂ V[N(Xyl)CMe=CC(=NXyl)CMeCH=CHCH=CMeC(=N)]							
V–N(1)	2.008(4)	N(3)–C(22)	1.365(5)	C(23)–C(24)	1.456(6)	C(26)–C(27)	1.341(6)
V–N(2)	1.957(4)	N(4)–C(23)	1.414(5)	C(24)–N(5)	1.281(5)	C(27)–C(28)	1.445(7)
V–N(3)	1.987(4)	N(4)–C(30)	1.322(5)	C(24)–C(25)	1.546(6)	C(28)–C(29)	1.370(6)
V–N(4)	2.103(4)	C(22)–C(23)	1.377(6)	C(25)–C(26)	1.490(6)	C(29)–C(30)	1.458(6)
N(1)–V–N(2)	130.8(2)	N(2)–V–N(3)	107.9(1)	N(3)–C(22)–C(23)	118.3(4)	C(23)–C(24)–N(5)	124.6(4)
N(1)–V–N(3)	117.2(1)	N(2)–V–N(4)	108.9(1)	N(4)–C(23)–C(22)	116.7(4)	C(24)–N(5)–C(23)	123.5(4)
N(1)–V–N(4)	97.0(1)	N(3)–V–N(4)	81.1(1)	N(4)–C(23)–C(24)	111.3(4)		
[(Me ₃ Si) ₂ N] ₂ VPh(pyr)							
V–N(1)	1.934(2)	V–N(3)	2.097(3)	N(1)–Si(3)	1.742(3)	N(2)–Si(1)	1.727(2)
V–N(2)	1.988(2)	V–C(13)	2.092(3)	N(1)–Si(4)	1.743(3)	N(2)–Si(2)	1.737(3)
N(1)–V–N(2)	121.6(1)	N(2)–V–N(3)	101.4(1)	V–N(1)–Si(3)	112.8(1)	V–N(2)–Si(1)	118.8(1)
N(1)–V–N(3)	111.4(1)	N(2)–V–C(13)	119.4(1)	V–N(1)–Si(4)	126.1(1)	V–N(2)–Si(2)	121.4(1)
N(1)–V–C(13)	108.0(1)	N(3)–V–C(13)	89.5(1)	Si(3)–N(1)–Si(4)	120.3(1)	Si(1)–N(2)–Si(2)	119.7(1)
[(Me ₃ Si) ₂ N] ₂ V(N=CPh ₂)(NCPh)							
V–N(1)	1.967(5)	V–N(4)	2.051(6)	N(1)–Si(1)	1.739(6)	N(2)–Si(3)	1.731(5)
V–N(2)	1.922(5)	N(3)–C(13)	1.284(8)	N(1)–Si(2)	1.728(6)	N(2)–Si(4)	1.739(5)
V–N(3)	1.817(5)	N(4)–C(26)	1.140(9)				
N(1)–V–N(2)	122.6(2)	N(2)–V–N(3)	116.5(2)	V–N(3)–C(13)	173.5(5)	N(3)–C(13)–C(14)	119.4(5)
N(1)–V–N(3)	115.3(2)	N(2)–V–N(4)	96.9(2)	V–N(4)–C(26)	172.2(6)	N(3)–C(13)–C(20)	121.4(6)
N(1)–V–N(4)	103.7(2)	N(3)–V–N(4)	92.7(2)				
[(Me ₃ Si) ₂ N] ₂ V(<i>o</i> -Me ₂ NCH ₂ C ₆ H ₄)							
V–N(1)	1.947(2)	V–N(3)	2.210(2)	N(1)–Si(1)	1.744(2)	N(2)–Si(3)	1.743(2)
V–N(2)	1.953(2)	V–C(13)	2.082(2)	N(1)–Si(2)	1.751(2)	N(2)–Si(4)	1.732(2)
N(1)–V–N(2)	119.24(8)	N(2)–V–N(3)	128.47(7)	V–C(13)–C(18)	112.1(2)	C(18)–C(19)–N(3)	109.3(2)
N(1)–V–N(3)	101.49(7)	N(2)–V–C(13)	106.67(8)	C(13)–C(18)–C(19)	116.3(2)	V–N(3)–C(19)	101.6(1)
N(1)–V–C(13)	115.49(8)	N(3)–V–C(13)	79.36(8)				
[(Me ₃ Si) ₂ N] ₂ V(η ² -BH ₄)(pyr)							
V–N(1)	1.908(2)	V–B	2.3054(4)	B–H(44)	1.18(4)	N(1)–Si(2)	1.749(2)
V–N(2)	1.986(2)	V–H(42)	1.94(3)	B–H(45)	1.08(6)	N(2)–Si(3)	1.741(2)
V–N(3)	2.099(2)	V–H(43)	1.85(4)	N(1)–Si(1)	1.750(2)	N(2)–Si(4)	1.738(2)
B–V–N(1)	113.91(6)	N(1)–V–N(2)	120.11(8)	V–H(42)–B	95(2)	H(42)–B–H(43)	109(2)
B–V–N(2)	118.85(5)	N(1)–V–N(3)	105.90(8)	V–H(43)–B	99(2)	H(44)–B–H(45)	112(3)
B–V–N(3)	91.86(5)	N(2)–V–N(3)	98.84(7)	H(42)–V–H(43)	57(2)		

variables refined against 3773 data for which $I > 3\sigma(I)$ were $R = 0.0432$, $R' = 0.0518$ and $S = 1.57$.

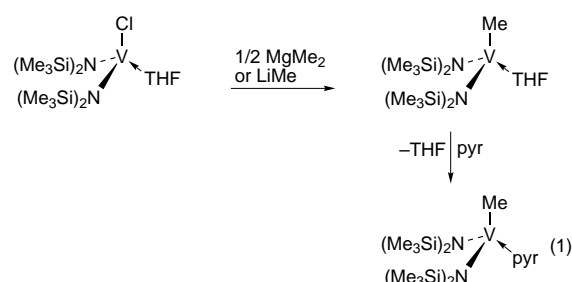
[(Me₃Si)₂N]₂V(η²-BH₄)(pyr). The material used for the X-ray investigation was prepared as described above, except only 1 equivalent of LiBH₄ was used per [(Me₃Si)₂N]₂VCl(THF). The data collection, preliminary treatments of the data, and solution of the structure were as described for [(Me₃Si)₂N]₂VPh(pyr). The space group $P2_1/c$ (no. 14) was uniquely defined by the systematic absences. The possibility of co-crystallized [(Me₃Si)₂N]₂VCl(pyr) was suggested by a negative thermal parameter for the boron. A model that constrained the coordinates and thermal parameters of a Cl to those of B refined to occupancies of 0.35 (Cl) and 0.65 (B). This model afforded more reasonable thermal parameters for the B/Cl and a significantly lower R value. The final residuals for 236 variables refined against 3123 data for which $I > 3\sigma(I)$ were $R = 0.0306$, $R' = 0.0422$ and $S = 1.63$.

CCDC reference number 186/756.

Results and Discussion

Synthesis of [(Me₃Si)₂N]₂VR(THF) (R = Me or 2-C₄H₃S)

Blue-green THF solutions of [(Me₃Si)₂N]₂VCl(THF)^{13,14} treated with a stoichiometric quantity of either MgMe₂ or LiMe gave royal blue mixtures from which the V^{III}–Me complex was isolated in yields of *ca.* 70% [equation (1)]. The substitution



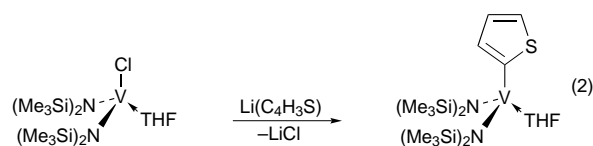
of chloride for methyl proceeded cleanly and we found no advantage in carrying out the reaction at lower temperatures. Although the compound is very sensitive to oxygen and water, its high crystallinity and indefinite stability at room temperature under dinitrogen facilitated the preparation of multi-gram quantities. The IR spectrum is similar to that of the chloride,¹⁴ showing strong bands for the bis(trimethylsilyl)amide at 1245 cm⁻¹ (δ_{sym} CH₃), 936 cm⁻¹ (ν_{asym} MNSi₂), 848 cm⁻¹ (ρ_{asym} CH₃), 781 cm⁻¹ (ν_{sym} MNSi₂),²⁵ as well as a band at 1012 cm⁻¹ (ν_{asym} C–O–C) indicating the presence of THF. The primary difference between the IR spectra of the V–Cl and V–Me species was a 46 cm⁻¹ blue shift of the ν_{asym} MNSi₂ in the methyl complex. A broad resonance centered at δ ca. 2.8 and a lower intensity signal at δ ca. 5.2 were observed in the ¹H NMR spectrum, but as with all of the other paramagnetic complexes reported here, the spectrum lacks informative structural data. The solution-state magnetic moment of 2.72 μ_{B} is consistent with a high spin d² electronic configuration.

Results of a single-crystal X-ray diffraction experiment have been previously communicated²⁶ and only the pertinent structural features will be mentioned here. The molecule is a four-co-ordinate monomer with V at the center of a distorted tetrahedron. The largest angle about the metal is between the bulky silylamides [N–V–N = 121.52(9)°]. The V–C bond length [2.095(4) Å] compares best to those in the V^V bimetallic Li-(μ -NSiBu^t₃)₂VMe₂ [2.057(8), 2.043(5) Å],²⁷ and the THF is co-ordinated with a normal dative interaction to the V^{III} [V–O 2.051(2) Å].

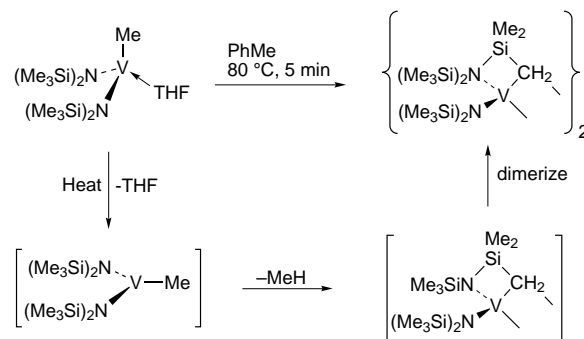
The compound [(Me₃Si)₂N]₂VMe(pyr) was prepared by adding 1 equivalent of pyr to [(Me₃Si)₂N]₂VMe(THF) [equation (1)], or in one step from [(Me₃Si)₂N]₂VCl(THF) by adding pyr to the reaction mixture subsequent to methylation. A medium intensity, characteristic absorption due to the pyr ring was observed in the IR spectrum at 1602 cm⁻¹. Under analogous conditions, the pyr adduct was more stable with respect to thermal decomposition than the THF adduct (see below), although the former compound also decomposed over several hours in solution at 80 °C to uncharacterized, paramagnetic product(s). In contrast to the reaction with pyr, the THF ligand in [(Me₃Si)₂N]₂VMe(THF) is not displaced by phosphines such as PMe₂Ph or PMe₃.

It is generally the case that β -hydrogen elimination requires a vacant metal co-ordination site.²⁸ Since the THF in the above species appeared to dissociate easily, the more robust [(Me₃Si)₂N]₂VCl(L) (L = pyr or lut) were prepared from [(Me₃Si)₂N]₂VCl(THF). However, for reasons that remain unclear, attempts at synthesizing even the Et derivative *i.e.* [(Me₃Si)₂N]₂VEt(L)} have been unsuccessful. It is noteworthy that both α - and β -hydrogen elimination decomposition processes operate in hydrocarbyl derivatives of the CpV^{III} (Cp = η -C₅H₅) fragment.^{29,30} Given that [(Me₃Si)₂N]₂VER [E = Se or Te; R = Si(SiMe₃)₃ or SiPh₃]¹ have pseudo-five-co-ordinate vanadium centers when apical C–H agostic interactions are taken into account, it is not inconceivable that species such as [(Me₃Si)₂N]₂VEt(L) may decompose by α - or β -hydrogen elimination to unstable intermediates even without prior dissociation of the L ligand.

The 2-thienyl complex, [(Me₃Si)₂N]₂V(2-C₄H₃S)(THF), was prepared as in equation (2) and isolated from hexanes as



blue-green crystals in 60% yield. Analytical data and the magnetic susceptibility ($\mu = 2.61 \mu_{\text{B}}$) were consistent with this formulation, as was the result of a hydrolysis experiment (10 equivalents of H₂O in C₆D₆) which yielded HN(SiMe₃)₂,



Scheme 1

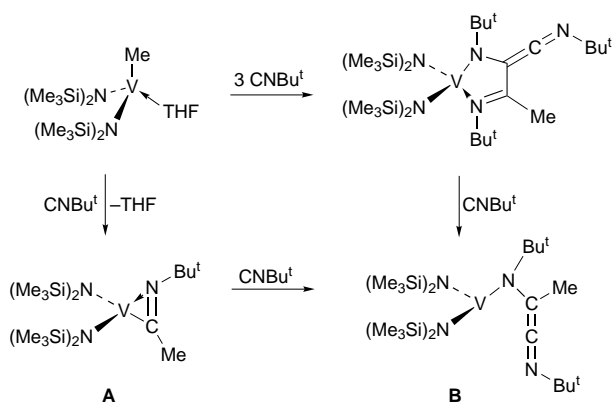
thiophene and THF in a 2:1:1 ratio, respectively, as the only observable products. The V–C(sp²) linkage appeared to be stable for prolonged periods in solution at room temperature in C₆D₆, however, as discussed below for the case of [(Me₃Si)₂N]₂VMe(THF), heating samples at 55 °C over several hours produced {[(Me₃Si)₂N]V(μ -CH₂SiMe₂NSiMe₃)}₂, thiophene and THF as the main products that were detected by ¹H NMR spectroscopy.

Reactivity of [(Me₃Si)₂N]₂VMe(THF)

Scheme 1 depicts the proposed mechanism for the thermal decomposition of the V^{III}–Me compound in hydrocarbon solvents. Thermolysis was carried out by heating a 0.03 M toluene solution of [(Me₃Si)₂N]₂VMe(THF) to 80 °C for 5 min, followed by standard work-up of the reaction mixture. Dimeric {[(Me₃Si)₂N]V(μ -CH₂SiMe₂NSiMe₃)}₂ was isolated as purple needles in 73% yield. This product was previously reported by Gambarotta and co-workers¹³ from the reaction of VCl₃·(THF)₃ with 3 equivalents of LiN(SiMe₃)₂ and its reactivity has been explored.^{31–33} As monitored by ¹H NMR spectroscopy in sealed NMR tubes, the thermolysis is very clean with the only resonances detected in thermolyzed samples attributable to the dimer and free THF. Qualitatively, the reaction proceeds with a half-life of ca. 1 h at 40 °C in C₆D₆ and is inhibited by excess THF. This latter point is consistent with loss of THF to generate the three-co-ordinate intermediate shown in Scheme 1. That the subsequent loss of methane is intramolecular is commensurate with observations of Andersen and co-workers on N(SiMe₃)₂ complexes of Group 4^{7,34} and f-block^{4,6} metals. It is noteworthy that attempts to isolate other derivatives of the form [(Me₃Si)₂N]₂VX(THF) (*e.g.* X = Et, CH₂SiMe₃, Ph, 4-Bu^tC₆H₄, Mes, NHR or OR; R = aryl) have not been successful, and in some cases good yields of the above dimer were isolated. This is reminiscent of the [(Me₃Si)₂N]₃UR system, where the hydride³⁵ and methyl³⁶ derivatives are accessible yet the putative [(Me₃Si)₂N]₃Uet is unstable towards loss of ethane.^{4,6} In the present case, it is likely that increased steric congestion about the vanadium lowers the barrier to dissociation of the THF, giving rise to decomposition processes analogous to that shown in Scheme 1.

The complex [(Me₃Si)₂N]₂VMe(THF) reacted rapidly in solution with substrates as diverse as CO, CO₂, CS₂, PhCN, CNC₆H₁₁ and ethylene. Unfortunately, no pure products were obtained from these reactions. The acetylenes PhCCPh and PhCCMe reacted to yield the previously mentioned dimer {[(Me₃Si)₂N]V(μ -CH₂SiMe₂NSiMe₃)}₂ in ca. 30% isolated yield. In these cases, as discussed above, it is likely that intermediate alkenyl species *i.e.* [(Me₃Si)₂N]₂VC(Ph)=CMePh and [(Me₃Si)₂N]₂VC(Me)=CMePh are unstable towards metalation of an amide ligand, as suggested for [(Me₃Si)₂N]₂V(CPh=CHPh)(THF).³⁷ The isocyanides CNBu^t and CNXyl reacted to yield tractable, paramagnetic complexes derived from the addition of the V–Me bond across the CNR triple bond.

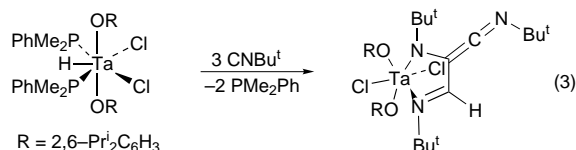
Treatment of [(Me₃Si)₂N]₂VMe(THF) with 3 equivalents of CNBu^t in cold hexanes initially gave a green solution that



Scheme 2

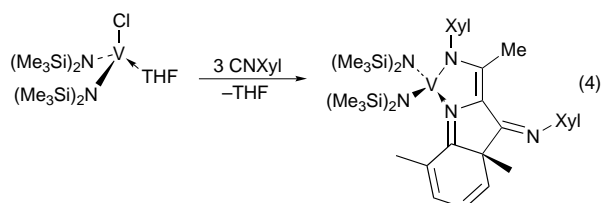
settled to golden red after warming to room temperature. After work-up, a complex of empirical formula $[(\text{Me}_3\text{Si})_2\text{N}]_2\text{V}[(\text{Me})(\text{CNBu}^t)_3]$ was isolated in 69% yield. X-Ray crystallography confirmed the connectivity shown in Scheme 2 in which 3 equivalents of CNBu^t have been coupled, with the original vanadium-bound methyl group exocyclic to the diazavanadacycle. While the ^1H NMR spectrum of the paramagnetic compound was devoid of any structural information, the IR spectrum was consistent with the result of the structural investigation in that no absorptions for THF were observed, and strong bands at 1987 and 1518 cm^{-1} may be attributed to vibrations of the keteneamine and $\text{C}=\text{N}$ bonds, respectively. A magnetic moment of $2.79\text{ }\mu_{\text{B}}$, measured in C_6D_6 , was consistent with the $+3$ oxidation state of the vanadium remaining unchanged.

Although the detailed mechanism of the reaction remains a matter of speculation, Scheme 2 shows an abbreviated, reasonable pathway for the reaction, in which all steps are well established in the literature.³⁸ An analogous reaction between a Ta^{V} hydride and 3 equivalents of CNBu^t has been reported by Rothwell and co-workers [equation (3)].^{39,40} Strong evidence for



the last step in Scheme 2, *i.e.* nucleophilic addition of a third equivalent of CNBu^t to the α -carbon of the amido keteneimine (intermediate **B**), comes by analogy from the reaction between the thoroxo keteneamine $\text{Cp}^*\text{TaCl}[\text{OC}(\text{C}=\text{O})\text{SiR}_3]$ [$\text{Cp}^* = \eta^5\text{-C}_5\text{Me}_5$; $\text{R}_3 = (\text{SiMe}_3)_3$ or Bu^tPh_2] and isocyanides and phosphines⁴¹ which yield isoelectronic metallacycles.

Three equivalents of CNXyl likewise reacted with $[(\text{Me}_3\text{Si})_2\text{N}]_2\text{VMe}(\text{THF})$ giving a green-red mixture that, over several minutes, gave way to a deep violet solution from which purple crystals of formula $[(\text{Me}_3\text{Si})_2\text{N}]_2\text{V}[(\text{Me})(\text{CNXyl})_3]$ were isolated in 75% yield. Elemental analysis and the magnetic susceptibility ($\mu = 2.81\text{ }\mu_{\text{B}}$) were in accord with 3 equivalents of CNXyl incorporated into the product. The IR spectrum had strong absorptions at 1636 and 1562 cm^{-1} indicative of $\text{C}=\text{N}$ and $\text{C}=\text{C}$ bonds. The valence bond formalisms drawn in equation (4)



reflect the results of a crystal-structure determination which is discussed above. Carbon-carbon bond formation between the

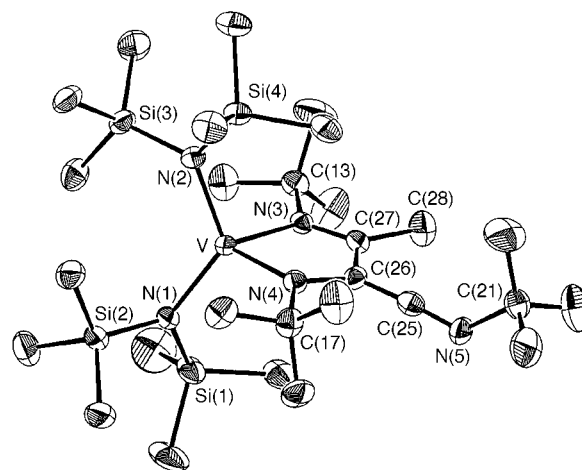
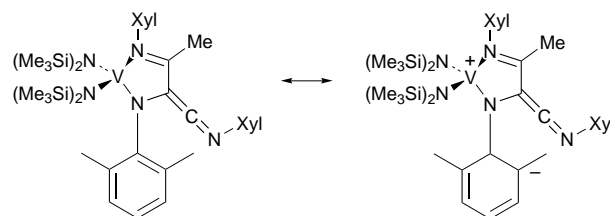
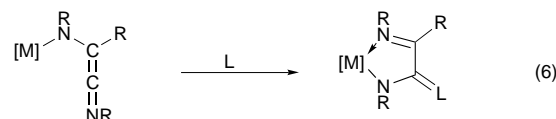
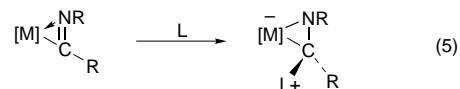


Fig. 1 An ORTEP drawing (50% ellipsoids) of $[(\text{Me}_3\text{Si})_2\text{N}]_2\text{V}[\text{Bu}^t\text{N}=\text{CMeC}(\text{C}=\text{N}\text{Bu}^t)\text{NBu}^t]$

2-position of a Xyl aryl ring and the neighboring carbon of a CNXyl group has been observed by Marks and co-workers⁴² in reactions between aryl isocyanides and thoroxo keteneimines. As in those instances, the accessibility of a resonance hybrid that posits an electrophilic aryl carbon in close proximity to the nucleophilic α -carbon of the keteneamine (below), results in facile $\text{C}-\text{C}$ bond formation.



In some cases, it has been seen that either intermediates or isolable species like **A** and **B** (Scheme 2) react with Lewis bases, as shown generally in equations (5) and (6).^{40,42-44} In the present



system this was not the case. For example, treating $[(\text{Me}_3\text{Si})_2\text{N}]_2\text{VMe}(\text{THF})$ with 2 equivalents of the isocyanides in the presence of 4 equivalents of PMe_2Ph still yielded the same diazavanadacycles in comparable yields. This fact, along with the observation that mixtures of the $\text{V}^{\text{III}}\text{-Me}$ compound and CNR in stoichiometric ratios of 1:1 or 1:2 still yielded the above products, albeit in diminished yields, suggest that the rate-determining step comes early in these processes. Since both reactions probably proceed through η^2 -iminoacyls (*e.g.* **A** in Scheme 2)⁴⁰ yet these compounds do not appear to be isolable, it is likely that formation of a species of this sort with the first equivalent of isocyanide is the slow step in these reactions.

An ORTEP⁴⁵ view of $[(\text{Me}_3\text{Si})_2\text{N}]_2\text{V}[\text{Bu}^t\text{N}=\text{CMeC}(\text{C}=\text{NBu}^t)\text{NBu}^t]$ is shown in Fig. 1; selected metrical data for this as well as other structurally characterized compounds are listed in Table 2. The vanadium-amide bond lengths are normal for $\text{N}(\text{SiMe}_3)_2$ complexes of V^{III} and both VNSi_2 units are virtually planar. The bond distances and angles within the diazavanadacycle are comparable to those reported for the above mentioned $(\text{RO})_2(\text{Cl})_2\text{Ta}[\text{Bu}^t\text{N}=\text{CMeC}(\text{C}=\text{NBu}^t)\text{NBu}^t]$ ($\text{R} = 2,6$ -

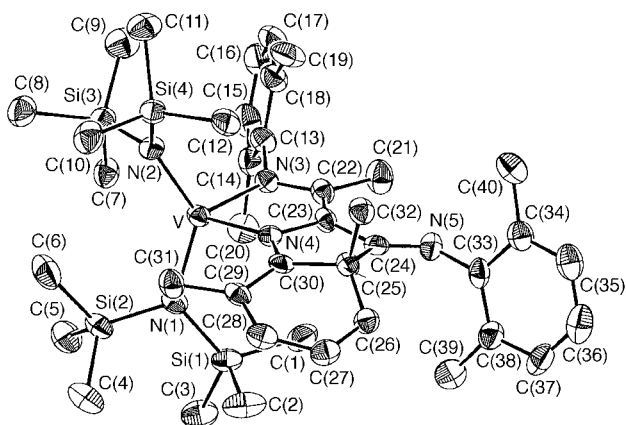


Fig. 2 An ORTEP drawing (50% ellipsoids) of $[(\text{Me}_3\text{Si})_2\text{N}]_2\text{V}-[\text{N}(\text{Xyl})\text{CMe}=\text{CC}(\text{=NXyl})\text{CMeCH}=\text{CHCH}=\text{CMeC}(\text{=N})]$

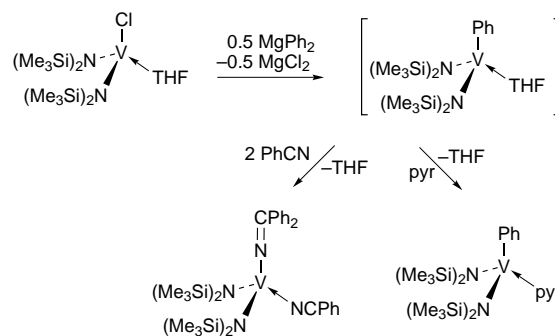
$\text{Pr}_2\text{C}_6\text{H}_3$) in accord with the 2,5-diazametallacyclopent-2-ene rings shown in equation (3) and Scheme 2. At 2.098(3) Å, the dative V–N(3) interaction is equivalent to the V–pyr distance in $[(\text{Me}_3\text{Si})_2\text{N}]_2\text{V}(\eta^2\text{-BH}_4)(\text{pyr})$ (see below), and is about 0.2 Å longer than the co-ordinate covalent V–N(4) bond of 1.921(2) Å. The N(3)–V–N(4) angle of 81.6(1)° is slightly larger than the 78.5(1)° in the tantalum case, probably due to increased steric congestion in the six-co-ordinate tantalum complex. A range of 101.9(1)–123.5(1)° is observed for the remaining angles about the vanadium, the largest angle being that between the two bulky silyl amides. The original vanadium-bound methyl group is bound directly to the metallacycle *via* a normal C–C single bond [C(27)–C(28) 1.507(5) Å]. Short C=C and C=N bond lengths as well as a virtually linear C=C=N array characterize the exocyclic keteneamine functionality [C(26)–C(25) 1.345(4), C(25)–N(5) 1.205(4) Å, C(26)–C(25)–N(5) = 171.7(3)°].

Fig. 2 shows an ORTEP view of the structure of the tris-(CNXyl) insertion product. Although the overall connectivity is more complex than in the CNBu⁺ case, the N₄ co-ordination environment around the vanadium is similar with the bite angle of the metallacycle being 81.1(6)°, and the remaining angles spanning the range 97.0(1)–130.8(2)°. An increase in V–N bond length of about 0.1 Å distinguishes the V–N(4) dative bond from the remaining co-ordinate covalent V–N interactions. The formation of the C(24)–C(25) single bond [1.546(6) Å] which results in the fused three-ring system also transforms the C(25)–C(30) aryl ring into a cyclohexa-1,3-diene. Analysis of the alterations in C–C bond lengths about the ring supports this view. The C(23)–C(24)–N(5) array that composed a linear keteneamine in the CNBu⁺ compound is reduced to an imine in the present case [C(23)–C(24) 1.456(6) Å; C(23)–C(24)–N(5) 124.6(4)°]. As a result of steric considerations, the C(13)–C(18) Xyl ring plane is oriented at an angle of 72.5° relative to the plane of the diazavanadacycle.

Vanadium(III) aryl derivatives

As illustrated in Scheme 3, treatment of THF solutions of $[(\text{Me}_3\text{Si})_2\text{N}]_2\text{VCl}(\text{THF})$ with 0.5 equivalent of MgPh_2 immediately gave deep blue solutions that act as sources of $'[(\text{Me}_3\text{Si})_2\text{N}]_2\text{VPh}'$. The putative $[(\text{Me}_3\text{Si})_2\text{N}]_2\text{VPh}(\text{THF})$ is evidently stable for prolonged periods in THF, and evaporation of solvent from the reaction mixture afforded a blue solid. However, on addition of hexanes to the material, the mixture quickly became purple and $\{[(\text{Me}_3\text{Si})_2\text{N}]_2\text{V}(\mu\text{-CH}_2\text{SiMe}_2\text{NSiMe}_3)_2\}_2$ was isolated in *ca.* 60% yield. In the absence of excess THF, it appears a decomposition like that in Scheme 1 readily occurs, a result that is somewhat surprising given the stability of $[(\text{Me}_3\text{Si})_2\text{N}]_2\text{V}(2\text{-C}_4\text{H}_9\text{S})(\text{THF})$.

Two reactions that lead to stable derivatives of the $[(\text{Me}_3\text{Si})_2\text{N}]_2\text{VPh}$ fragment are shown in Scheme 3. The pyr adduct



Scheme 3

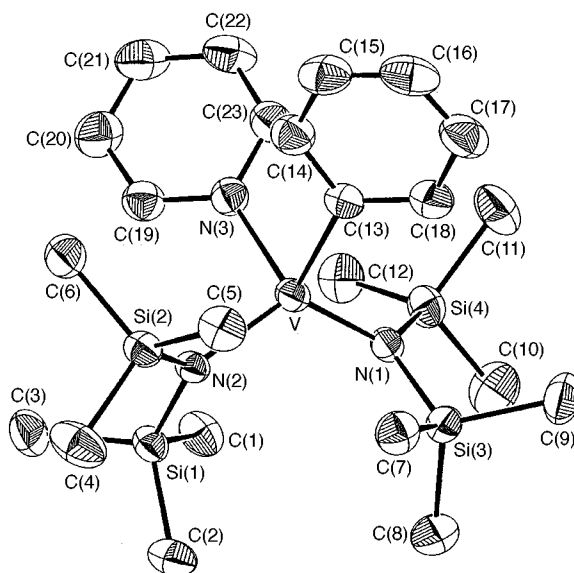


Fig. 3 An ORTEP drawing (50% ellipsoids) of $[(\text{Me}_3\text{Si})_2\text{N}]_2\text{VPh}(\text{pyr})$

may be isolated in 60% yield as green crystals. It was characterized by elemental analysis, IR spectroscopy ($\nu_{\text{pyr}} = 1603 \text{ cm}^{-1}$), magnetic susceptibility ($\mu = 2.75 \mu_{\text{B}}$) and X-ray crystallography. An ORTEP view of the structure is shown in Fig. 3. As expected, the largest angle about the vanadium is between the bulky silyl amides [N(1)–V–N(2) = 121.6(1)°], whereas the smallest angle is subtended between the Ph and pyr ligands [C(13)–V–N(3) = 89.5(1)°], whose respective planes are skewed at 119° with respect to each other. As delineated in the Experimental section, a disorder on the order of 25% between the two ligands negates a discussion of distinct V–Ph and V–pyr bond lengths. Nevertheless, both refined distances of *ca.* 2.1 Å are reasonable when compared with other pyr and Ph complexes of V^{III}.^{46–48} The two V–amide bond lengths are slightly different [V–N(1) 1.934(2), V–N(2) 1.988(2) Å]. This is explained by noting that different degrees of rotation about the V–amide bonds, with respect to the V–N(3)–C(13) plane, render the amides inequivalent. More specifically, the Si(2)–N(2)–V–C(13) torsion angle of 3.5(2)° posits the Si(2) trimethylsilyl group rather close to the Ph group. Whereas for the N(1) amide, the analogous torsion angle [Si(4)–N(1)–V–N(3) 7.6(2)°] allows the Si(4) trimethylsilyl to lie slightly farther from the pyridine ligand.

Addition of 3 equivalents of PhCN to a blue solution of $[(\text{Me}_3\text{Si})_2\text{N}]_2\text{VPh}(\text{THF})$ afforded on work-up burgundy crystals of formula $[(\text{Me}_3\text{Si})_2\text{N}]_2\text{V}[(\text{Ph})(\text{PhCN})_2]$ in 66% yield. The material was paramagnetic with a solution-state magnetic moment of 2.67 μ_{B} . Infrared spectroscopy indicated two different types of CN functionalities with absorptions observed at 2236 and 1596 cm^{-1} . X-Ray crystallography (Fig. 4) confirmed the material to be the V^{III} azaalkenyldiene (V–N=CR₂)⁴⁹ drawn in Scheme 3. Since the original vanadium-bound phenyl group

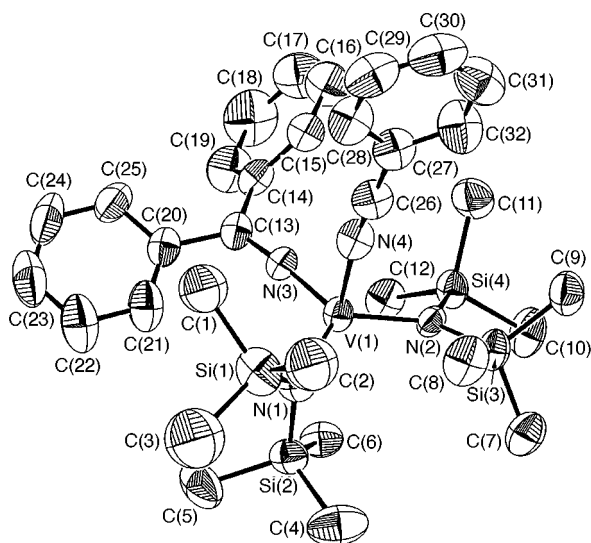
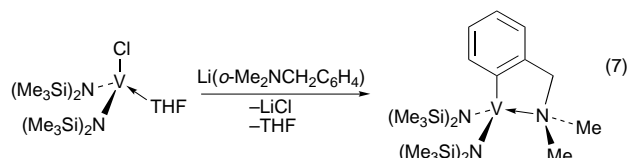


Fig. 4 An ORTEP drawing (50% ellipsoids) of $[(\text{Me}_3\text{Si})_2\text{N}]_2\text{V}(\text{N}=\text{CPh}_2)(\text{NCPh})$

has undergone a 1,3-shift to the carbon atom of a PhCN,⁵⁰ it is likely that the reaction proceeds by the substitution of THF with PhCN, followed by Ph migration to give intermediate $[(\text{Me}_3\text{Si})_2\text{N}]_2\text{V}-\text{N}=\text{CPh}_2$, which is then trapped by an additional equivalent of PhCN to yield the isolated product.

An ORTEP drawing showing the solid-state structure of $[(\text{Me}_3\text{Si})_2\text{N}]_2\text{V}(\text{N}=\text{CPh}_2)(\text{NCPh})$ is shown in Fig. 4. The data are relatively poor (see Experimental section), but serve to verify connectivity within this paramagnetic molecule. The distortion of the N_4 co-ordination environment about the vanadium is such that the $\text{N}(3)-\text{V}-\text{N}(4)$ angle of $92.7(2)^\circ$ is the smallest and the $\text{N}(1)-\text{V}-\text{N}(2)$ angle of $122.6(2)^\circ$ is the largest. At $2.051(6)$ Å, the dative interaction between the nitrile and the metal is slightly longer than the co-ordinate covalent V–amide bond lengths. Significantly shorter is the V–N(3) distance of $1.817(5)$ Å that characterizes the V–azaalkenyldiene linkage. While the bond length is not as short as those observed in vanadium(III) imides ($\text{V}=\text{NR}$ ca. 1.7 Å),^{29,30} it is shorter than expected for a $\text{V}^{\text{III}}-\text{N}$ single bond suggesting there is some delocalization along the $\text{V}-\text{N}=\text{CPh}_2$ array. This is consistent with both the $\text{V}-\text{N}(3)-\text{C}(13)$ and $\text{V}-\text{N}(4)-\text{C}(26)$ angles being statistically equivalent [$173.5(5)$ and $172.2(6)^\circ$, respectively] and close to linear.

The kinetic stability of five-membered chelate rings and of metal aryls that have an *ortho* substituent capable of chelation to a metal center has been known for years. Both of these requirements are met by the *o*-dimethylaminomethylphenyl ligand and it has thus been used widely in organometallic chemistry.⁵¹ In the present case, reaction of $[(\text{Me}_3\text{Si})_2\text{N}]_2\text{VCl}(\text{THF})$ with $\text{Li}(o\text{-Me}_2\text{NCH}_2\text{C}_6\text{H}_4)$ in THF resulted in a rapid reaction that gave the chelated arylamine shown in equation (7). The deep blue product was formed, exclusively,



and after extraction of the complex with hexanes from LiCl the solvent may be stripped off to afford pure material as a powder. Alternatively, large blue crystals were obtained by crystallization from hexanes. Elemental analysis was consistent with the formulation in equation (7) and a magnetic moment of $2.77 \mu_{\text{B}}$ in solution was in accord with the $\text{V}^{\text{III}} d^2$ high-spin electronic configuration. The greater stability of the V–C bond in this

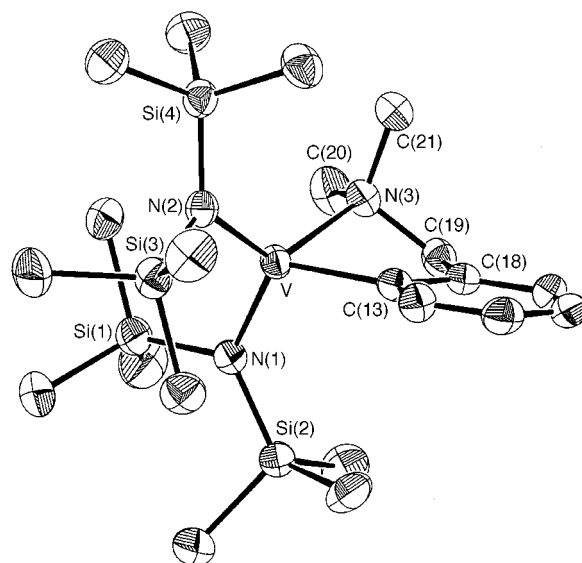


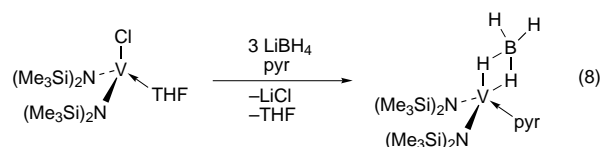
Fig. 5 An ORTEP drawing (50% ellipsoids) of $[(\text{Me}_3\text{Si})_2\text{N}]_2\text{V}(o\text{-Me}_2\text{NCH}_2\text{C}_6\text{H}_4)$

system was evidenced by a lack of reactivity of $[(\text{Me}_3\text{Si})_2\text{N}]_2\text{V}(o\text{-Me}_2\text{NCH}_2\text{C}_6\text{H}_4)$ with PhCN, PhCCMe or Me_3SiCCH . A color change from blue to green was observed when the aryl was treated with an excess of CO (1 atm), however a pure product was not isolated from the reaction mixture.

The result of a structural determination is shown in Fig. 5. The *ipso* carbon of the aryl and the amine nitrogen are chelated to the vanadium with an angle of $79.36(8)^\circ$. As a result, the largest angle about the metal center is the $\text{N}(2)-\text{V}-\text{N}(3)$ angle of $128.47(7)^\circ$, with the angle between the bulky silyl amides being $119.24(8)^\circ$. The ligand–metal bond lengths of $1.950(3)$ Å for the amides ($\text{V}-\text{N}_{\text{ave}}$), $2.082(2)$ Å for $\text{V}-\text{C}(13)$ and $2.210(2)$ Å for $\text{V}-\text{N}(3)$ are in the expected ranges.

Vanadium(III) tetrahydroborate

In an attempt to generate a V–H functionality, $[(\text{Me}_3\text{Si})_2\text{N}]_2\text{VCl}(\text{THF})$ was reacted with LiBH_4 over several hours, and then pyr was added to the reaction mixture. The product of this reaction was the pyridine adduct of a V^{III} –tetrahydroborate in 41% yield [equation (8)]. The IR spectrum of the complex



possessed a medium intensity absorption at 1605 cm^{-1} that indicated the presence of co-ordinated pyr, and analytical data as well as the magnetic susceptibility ($\mu = 2.78 \mu_{\text{B}}$) were consistent with the proposed formulation. Bands in the IR spectrum also clearly implicated the material as a V–BH₄ complex, with the pattern of absorptions most consistent with an η^2 hapticity for the tetrahydroborate ligand. For example, a pair of medium intensity absorptions at 2453 and 2402 cm^{-1} may be ascribed to the B–H_i stretching (A_1 , B_1), and a broader absorption at 2141 cm^{-1} is most likely due to the B–H_b stretching (A_1 , B_2).⁵² As is often the case in reactions of this sort,⁵² an excess of LiBH_4 was required to affect complete substitution of the chloride ligand. In fact, the co-crystallization of $[(\text{Me}_3\text{Si})_2\text{N}]_2\text{VCl}(\text{pyr})$ and $[(\text{Me}_3\text{Si})_2\text{N}]_2\text{V}(\eta^2\text{-BH}_4)(\text{pyr})$ in a 0.35:0.65 ratio (as determined by X-ray crystallography) was observed when the reaction in equation (8) was carried out with only 1 equivalent of LiBH_4 . In the absence of added pyr, we experienced difficulty in isolating a product. Although, in a similar reaction using

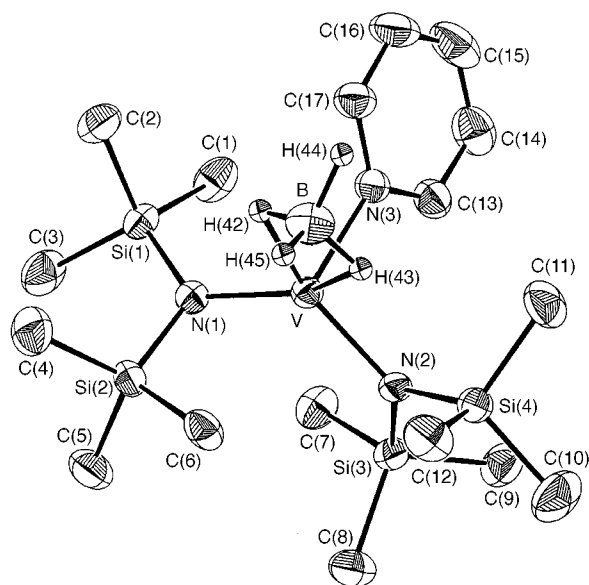


Fig. 6 An ORTEP drawing (50% ellipsoids) of $[(\text{Me}_3\text{Si})_2\text{N}]_2\text{V}(\eta^2\text{-BH}_4)(\text{pyr})$

8 equivalents of NaBH_4 , $[(\text{Me}_3\text{Si})_2\text{N}]_2\text{V}(\eta^2\text{-BH}_4)(\text{THF})$ was isolated in 6% yield.¹⁴ Attempts to use $[(\text{Me}_3\text{Si})_2\text{N}]_2\text{V}(\eta^2\text{-BH}_4)(\text{pyr})$ as a precursor for a vanadium hydride by abstraction of BH_3 with excess pyr, Me_3N or Me_3P all resulted in no reaction.

Fig. 6 shows an ORTEP drawing of $[(\text{Me}_3\text{Si})_2\text{N}]_2\text{V}(\eta^2\text{-BH}_4)(\text{pyr})$, the structure having confirmed a η^2 bonding mode for the BH_4 ligand. As mentioned above and described in the Experimental section, co-crystallized $[(\text{Me}_3\text{Si})_2\text{N}]_2\text{VCl}(\text{pyr})$ was present in ca. 35%, as estimated by the refined occupancy of a chlorine atom constrained to lie at the same position as the boron. The high quality of the structure (all hydrogen atoms were located and their positions refined) indicates that these species are isostructural. Despite the dihedral angle between the BH_2 (terminal) and $\text{BVN}(3)$ planes being close to 0° [e.g. $\text{N}(3)\text{-V-B-H}(44) -2(2)$, $\text{N}(3)\text{-V-B-H}(45) -179(3)^\circ$], a 47° tilt of the pyr ring plane with respect to the BH_2 (terminal) plane makes for a small $\text{B-V-N}(3)$ angle of $91.86(5)^\circ$. The angle subtended between the silyl amide ligands $[\text{N}(1)\text{-V-N}(2) 120.11(8)^\circ]$ is the largest about the vanadium. The orientation of the bridging $\text{H}(43)$ atom roughly along the $\text{V-N}(2)$ amide bond [$\text{H}(43)\text{-B-V-N}(2) 11(2)^\circ$], is the probable explanation for the slightly longer $\text{V-N}(2)$ bond length of $1.986(2) \text{ \AA}$, versus a value of $1.908(2) \text{ \AA}$ for the $\text{V-N}(1)$ bond. Equivalent V-H_b [$\text{V-H}(42) 1.94(3)$, $\text{V-H}(43) 1.85(4) \text{ \AA}$] and B-H_b [$\text{B-H}(42) 1.08(4)$, $\text{B-H}(43) 1.12(4) \text{ \AA}$] interactions suggest a symmetrical η^2 orientation of the BH_4 ligand. In contrast, the BH_4 ligand in the solid-state structure of $[(\text{Me}_3\text{Si})_2\text{N}]_2\text{V}(\text{BH}_4)(\text{THF})$ is distorted towards a co-ordination mode intermediate between η^1 and η^2 .¹⁴

Acknowledgements

We thank the National Science Foundation for support and the Alfred P. Sloan Foundation for a fellowship (to J. A.).

References

- C. P. Gerlach and J. Arnold, *Inorg. Chem.*, 1996, **35**, 5770.
- P. Berno, S. Gambarotta and D. Richeson, in *Comprehensive Organometallic Chemistry II*, eds. E. D. Abel, F. G. A. Stone and G. Wilkinson, Elsevier, New York, 1995, vol. 5, p.1.
- C. R. Bennett and D. C. Bradley, *J. Chem. Soc., Chem. Commun.*, 1974, 29.
- S. J. Simpson, H. W. Turner and R. A. Andersen, *J. Am. Chem. Soc.*, 1979, **101**, 7728.
- S. J. Simpson and R. A. Andersen, *Inorg. Chem.*, 1981, **20**, 3627.
- S. J. Simpson, H. W. Turner and R. A. Andersen, *Inorg. Chem.*, 1981, **20**, 2991.
- R. P. Planalp, R. A. Andersen and A. Zalkin, *Organometallics*, 1983, **2**, 16.
- W. Seidel and G. Kreisel, *Z. Chem.*, 1974, **14**, 25.
- W. Seidel and G. Kreisel, *Z. Anorg. Allg. Chem.*, 1977, **435**, 146.
- M. Vivanco, J. Ruiz, C. Floriani, A. Chiesi-Villa and C. Rizzoli, *Organometallics*, 1993, **12**, 1794.
- M. Vivanco, J. Ruiz, C. Floriani, A. Chiesi-Villa and C. Rizzoli, *Organometallics*, 1993, **12**, 1802.
- J. Ruiz, M. Vivanco, C. Floriani, A. Chiesi-Villa and C. Rizzoli, *Organometallics*, 1993, **12**, 1811.
- P. Berno, R. Minhas, S. Hao and S. Gambarotta, *Organometallics*, 1994, **13**, 1052.
- P. Berno, M. Moore, R. Minhas and S. Gambarotta, *Can. J. Chem.*, 1996, **74**, 1930.
- R. A. Andersen and G. Wilkinson, *J. Chem. Soc., Dalton Trans.*, 1977, 809.
- J. T. B. H. Jastrzebski, G. Van Koten, M. F. Lappert, P. C. Blake and D. R. Hankey, in *Inorganic Syntheses*, ed. H. D. Kaesz, Wiley, New York, 1989, vol. 26, p. 150.
- L. Engman and M. P. Cava, *Organometallics*, 1982, **1**, 470.
- D. F. Evans, *J. Chem. Soc.*, 1959, 2003.
- E. M. Schubert, *J. Chem. Educ.*, 1992, **69**, 62.
- SMART Area-Detector Software Package, Siemens Industrial Automation, Inc., Madison, WI, 1993.
- SAINT: SAX Area-Detector Integration Program, version 4.024, Siemens Industrial Automation, Inc., Madison, WI, 1994.
- TEXSAN: Crystal Structure Analysis Package, Molecular Structure Corporation, Houston, TX, 1992.
- D. T. Cromer and J. T. Waber, *International Tables for X-ray Crystallography*, The Kynoch Press, Birmingham, 1974, vol. IV, Table 2.2B.
- D. T. Cromer and J. T. Waber, *International Tables for X-ray Crystallography*, The Kynoch Press, Birmingham, 1974, vol. IV, Table 2.3.1.
- E. C. Alyea, D. C. Bradley and R. G. Copperthwaite, *J. Chem. Soc., Dalton Trans.*, 1972, 1580.
- C. P. Gerlach and J. Arnold, *Organometallics*, 1996, **15**, 5260.
- J. de With, A. D. Horton and A. G. Orpen, *Organometallics*, 1990, **9**, 2207.
- J. P. Collman, L. S. Hegedus, J. R. Norton and R. G. Finke, *Principles and Applications of Organotransition Metal Chemistry*, University Science Books, Mill Valley, CA, 1987.
- B. Hessen, J.-K. F. Buijink, A. Meetsma and J. H. Teuben, *Organometallics*, 1993, **12**, 2268.
- J.-K. F. Buijink, K. R. Kloetstra, A. Meetsma and J. H. Teuben, *Organometallics*, 1996, **15**, 2523.
- P. Berno and S. Gambarotta, *Organometallics*, 1994, **13**, 2569.
- P. Berno and S. Gambarotta, *J. Chem. Soc., Chem. Commun.*, 1994, 2419.
- P. Berno and S. Gambarotta, *Angew. Chem., Int. Ed. Engl.*, 1995, **34**, 822.
- R. P. Planalp and R. A. Andersen, *Organometallics*, 1983, **2**, 1675.
- H. W. Turner, S. J. Simpson and R. A. Andersen, *J. Am. Chem. Soc.*, 1979, **101**, 2782.
- H. W. Turner, R. A. Andersen, D. H. Templeton and A. Zalkin, *Inorg. Chem.*, 1979, **18**, 1221.
- M. Moore, S. Gambarotta, G. Yap, L. M. Liable-Sands and A. L. Rheingold, *Chem. Commun.*, 1997, 643.
- L. D. Durfee and I. P. Rothwell, *Chem. Rev.*, 1988, **88**, 1059.
- J. R. Clark, P. E. Fanwick and I. P. Rothwell, *J. Chem. Soc., Chem. Commun.*, 1993, 1233.
- J. R. Clark, P. E. Fanwick and I. P. Rothwell, *Organometallics*, 1996, **15**, 3232.
- N. S. Radu, M. P. Engeler, C. P. Gerlach and T. D. Tilley, *J. Am. Chem. Soc.*, 1995, **117**, 3621.
- K. G. Molloy, P. J. Fagan, J. M. Manriquez and T. J. Marks, *J. Am. Chem. Soc.*, 1986, **108**, 56.
- B. K. Campion, R. H. Heyn and T. D. Tilley, *Organometallics*, 1993, **12**, 2584.
- J. Arnold, T. D. Tilley, A. L. Rheingold, S. J. Geib and A. M. Arif, *J. Am. Chem. Soc.*, 1989, **111**, 149.
- C. K. Johnson, ORTEP, Report ORNL-5138, Oak Ridge National Laboratory, Oak Ridge, TN, 1976.
- E. Solari, S. De Angelis, C. Floriani, A. Chiesi-Villa and C. Rizzoli, *Inorg. Chem.*, 1992, **31**, 96.
- J.-M. Rosset, C. Floriani, M. Mazzanti, A. Chiesi-Villa and C. Guastini, *Inorg. Chem.*, 1990, **29**, 3991.

- 48 A. R. Wills, P. G. Edwards, M. Harman and M. B. Hursthouse, *Polyhedron*, 1989, **8**, 1457.
- 49 H. Werner, W. Knaup and M. Dziallas, *Angew. Chem., Int. Ed. Engl.*, 1987, **26**, 248.
- 50 For other examples of nitrile insertion into early metal-carbon σ bonds as well as references for different routes to $\text{N}=\text{CR}_2$ complexes, see the following and refs. therein: C. Kreuder and R. F. Jordan, *Organometallics*, 1995, **14**, 2993; B. Temme, G. Erker, R. Fröhlich and M. Grehl, *J. Chem. Soc., Chem. Commun.*, 1994, 1713;
- M. Bochmann, L. M. Wilson, M. B. Hursthouse and M. Motevalli, *Organometallics*, 1988, **7**, 1148; G. Erker, W. Frömbeg, C. Krüger and E. Raabe, *J. Am. Chem. Soc.*, 1988, **110**, 2400.
- 51 See the following and refs. therein: H. C. L. Abbenhuis, R. van Belzen, D. M. Grove, A. J. A. Klomp, G. P. M. van Mier, A. L. Spek and G. van Koten, *Organometallics*, 1993, **12**, 210.
- 52 T. J. Marks and J. R. Kolb, *Chem. Rev.*, 1977, **77**, 263.

Received 21st July 1997; Paper 7/05238C